Chemistry and Physics of Lipids 190 (2015) 43–50

Contents lists available at ScienceDirect

Chemistry and Physics of Lipids

journal homepage: www.elsevier.com/locate/chemphyslip

Selective deuteration for molecular insights into the digestion of medium chain triglycerides

Stefan Salentinig[a,**], Nageshwar Rao Yepuri[b], Adrian Hawley[c], Ben J. Boyd[a], Elliot Gilbert[d], Tamim A. Darwish[b,*]

[a] Drug Delivery, Disposition and Dynamics, Monash Institute of Pharmaceutical Sciences, Monash University (Parkville Campus), 381 Royal Parade, Parkville, VIC 3052, Australia
[b] National Deuteration Facility, Australian Nuclear Science and Technology Organisation, Locked Bag 2001, Kirrawee DC, NSW 2232, Australia
[c] SAXS/WAXS Beamline, Australian Synchrotron, 800 Blackburn Rd, Clayton, VIC 3168, Australia
[d] Bragg Institute, Australian Nuclear Science and Technology Organisation, Locked Bag 2001, Kirrawee DC, NSW 2232, Australia

ARTICLE INFO

Article history:
Received 26 May 2015
Received in revised form 29 June 2015
Accepted 30 June 2015
Available online 4 July 2015

Keywords:
Selective deuteration
Medium chain triglycerides
Pancreatic lipase
Enzymatic interesterification
Tricaprin
Monocaprin
Capric acid
Deuterated lipids

ABSTRACT

Medium chain triglycerides (MCTs) are a unique form of dietary fat that have a wide range of health benefits. They are molecules with a glycerol backbone esterified with medium chain (6–12 carbon atoms) fatty acids on the two outer (*sn-1* and *sn-3*) and the middle (*sn-2*) positions. During lipid digestion in the gastrointestinal tract, pancreatic lipase stereoselectively hydrolyses the ester bonds of these triglycerides on the *sn-1* and *sn-3* positions resulting in *sn-2* monoglyceride and fatty acids as major products. However, the *sn-2* monoglycerides are thermodynamically less stable than their *sn-1/3* counterparts. Isomerization or fatty acid migration from the *sn-2* monoglyceride to *sn-1/3* monoglyceride may occur spontaneously and would lead to glycerol and fatty acid as final products. Here, tricaprin (C10) with selectively deuterated fatty acid chains was used for the first time to monitor chain migration and the stereoselectivity of the pancreatic lipase-catalyzed hydrolysis of ester bonds. The intermediate and final digestion products were studied using NMR and mass spectrometry under biologically relevant conditions. The hydrolysis of the *sn-2* monocaprin to glycerol and capric acid did not occur within biologically relevant timescales and fatty acid migration occurs only in limited amounts as a result of the presence of undigested diglyceride species over long periods of time in the digestion medium. The slow kinetics for the exchange of the *sn-2* fatty acid chain and the stereoselectivity of pancreatic lipase on MCTs is relevant for industrial processes that involve enzymatic interesterification and the production of high-value products such as specific structured triacylglycerols, confectionery fats and nutritional products.

1. Introduction

Dietary triglycerides are water-insoluble lipids, which are converted to more polar products during digestion for absorption. The glycerol backbone of the triglycerides allows three stereochemically distinct fatty acids positions: the two outer (*sn-1*,*sn-3*) and the middle position (*sn-2*). Digestion catalyzed pancreatic lipase hydrolyzes triglycerides stereospecifically to *sn-2* monoglyceride and free fatty acids (Borgström, 1964). These components are physiologically-relevant as only the fatty acid at the *sn-2* position can be absorbed intact as *sn-2* monoglyceride whereas the fatty acids at *sn-1,3* positions in the triglycerides are absorbed as free fatty acids that metabolize independently. Fatty acids and monoglycerides enter the enterocytes as monomers. There they are resynthesized to triglycerides by the action of the triglyceride synthetase complex (Voet and Voet, 1995). Some *sn-2* monoglyceride might ultimately serve as the backbone for gut or liver phospholipids, exerting downstream influence on lipid metabolism (Hayes, 2001). However, the *sn-2* monoglycerides are thermodynamically less stable than their *sn-1*/3counterparts. Isomerization or fatty acid migration from the *sn-2* monoglyceride to *sn-1* or *sn-3* monoglyceride may occur spontaneously and would lead to glycerol and fatty acid as final products. More than 30% acyl migration was found in *sn-1,2* diglycerides after 24 h at 37 °C (Kodali et al., 1990). The resulting equilibrium distribution in long chain monoglycerides (fatty acid chain length >14) comprises of 9% *sn-2* and 91% *sn-1*, with shorter chain fatty acids migrating faster

* Corresponding author.
** Corresponding author.
E-mail addresses: stefan.salentinig@gmail.com (S. Salentinig), tamim.darwish@ansto.gov.au (T.A. Darwish).

http://dx.doi.org/10.1016/j.chemphyslip.2015.06.007
0009-3084/

than longer chain fatty acids (Laszlo et al., 2008; Compton et al., 2007; Boswinkel et al., 1996).

The formation of *sn-2* monoglyceride in equilibrium conditions is enhanced up to 80% yield by the presence of self-assembled structures (Kodali et al., 1990; Holmberg and Osterberg, 1988; Holmberg and Österberg, 1990; Mazur et al., 1993). This is biologically-relevant, as these structures such as mixed micelles and more complex liquid crystalline structures are observed in monoglyceride/free fatty acid/bile salt mixtures (Hernell et al., 1990; Hofmann and Borgström, 1964; Mazer et al., 1980; Schurtenberger et al., 1985; Salentinig et al., 2014) and during the *in-vitro* digestion of triglyceride emulsions (Salentinig et al., 2011) and milk fat (Salentinig et al., 2013; Salentinig et al., 2015). These structures also form the basis for the transport and absorption of lipids and support the solubilisation and absorption of oil-soluble food components (*e.g.*, carotenes, vitamin A, D, E, and K) in the aqueous system of the gastrointestinal tract (Salentinig et al., 2014; Salentinig et al., 2011; Salentinig et al., 2013; Salentinig et al., 2010). Compared to molecular transport, micelles and vesicles enhance the number of fatty acid and monoglyceride molecules available for uptake by the enterocytes. From a monomeric point of view, fatty acid is transferred 3-fold faster than the corresponding monoglyceride under pH conditions of the small intestine (Narayanan and Storch, 1996). The size of the fatty acid is extremely important as the physiological effects of medium-chain fatty acids are distinctly different from the long-chain fatty acids more commonly found in our diet. Medium-chain triglycerides (MCTs) are generally considered a good biologically inert source of energy that humans find relatively easy to metabolize and are a common excipient in pharmaceutical lipid-based formulations (Bach and Babayan, 1982). Until the early 1980s, MCTs were predominantly available only as a constituent of butter, coconut oil, and other natural sources. However, since that date, processes have been developed to produce them in large quantities to be used primarily for therapeutic application in a number of conditions and for the treatment of disorders of lipid absorption. Thus a complete understanding of the MCT digestion process on the molecular level is imperative. Knowledge and understanding of how these food and supplement components are treated and utilized during the digestion process opens opportunities for functional food products that may help to avoid or cure health issues including obesity, vitamin malabsorption, the risk of coronary heart disease and cancer (Austin, 1991; Unger and Zhou, 2001; Katan, 2000). However, there is a lack of information on the stereoselectivity and fatty acid chain dynamics in digestion processes catalysed by pancreatic lipase. This information is also important in industrial processes that utilize lipase technology for the modification of oils and fats to produce high-value added products, such as cocoa butter equivalents, human milk fat substitutes, and other specific-structured lipids. Enzymatic interesterification is a catalytic reaction that occurs when an enzyme is introduced into oil and rearranges the fatty acids on the glycerol backbone of a triglyceride (Xu, 2000). For example, tripalmitin treated with oleic acid in the presence of 1,3-specific pancreatic lipase gives products where the palmitate is retained at the *sn-2* position, whereas oleate is introduced at *sn-1* and *sn-3*, producing a human milk fat substitute such as Betapol. In practice, pure starting materials are not used (Akoh and Xu, 2002).

Here we report the synthesis of selectively deuterated tricaprin, a medium chain length triglyceride, to study the intermediate and final products of the *in situ* digestion by pancreatic lipase using ^{1}H and ^{2}H NMR and mass spectrometry (MS) under biologically relevant conditions (pH, T, bile salt and lipase concentration). The use of selective deuteration provides a direct method to identify unequivocally the final products of digestion of this symmetrical triglyceride using mass spectrometry. A combination of (i) fully-protonated tricaprin; (ii) tricaprin with fully-deuterated fatty acids on the *sn-1/3* positions, a deuterium atom on the *C2* position of the glycerol backbone, and non-deuterated fatty acid on position *sn-2*; and (iii) tricaprin with the fully deuterated fatty acid on the *sn-2* position and non-deuterated fatty acid on the *sn-1/3* were used to investigate the stereoselectivity of the lipase action, fatty acid chain migration and enable product determination with mass spectrometry. In mass spectrometry, deuterated adducts occur at higher m/z values compared to their hydrogenated counterparts as a result of the mass difference of deuterium and hydrogen. As a consequence, mass spectra from the hydrolysis of the deuterated components provides detailed *qualitative* information on the stereochemistry of the hydrolysis reaction. In the absence of deuteration, mass spectrometry would not be able to determine the identity of the structural isomers of the digested products due to the similarity in the mass values of the different isomers of monoglycerides or diglycerides. For NMR, deuteration provides another nucleus (*i.e.*, ^{2}H) and frequency dimension, which allows cleaner spectral windows to be probed for changes when a mixture of hydrogen containing reagents is used: the ^{2}H labeled fatty acid chains of interest in the triglycerides can be solely probed without any interference from the ^{1}H signals of the other components. This approach allows direct observation of the signals during the digestion process and allows monitoring of the appearance and disappearance of signals and assists in confirming the identity of the final digestion products that are determined by mass spectrometry.

2. Materials and methods

2.1. Materials

Selectively-deuterated tricaprin with two fully-deuterated capric acid chains on the *sn-1* and *sn-3* positions and one deuterium atom on the *C2* position of the glycerol backbone, as well as deuterated tricaprin with fully-deuterated fatty acid chain on the *sn-2* position were synthesized as described below. Tricaprin ($C_{33}H_{62}O_{6,}$ >98%) was purchased from Tokyo Chemical Industry Co., Ltd., Tokyo, Japan. Bile salt (sodium taurodeoxycholate >95%), NaOH, NaOD, HCl and DCl (p.a. grade) were purchased from Sigma Aldrich (St. Louis, MO, USA). Pancreatin extract (USP grade pancreatin activity) was from Southern Biologicals (Nunawading, Victoria, Australia). D_2O (99.8%) was supplied by AECL (Ontario, Canada). Ultra-pure water (resistivity >18 MΩ cm) was used for the preparation of all samples.

The deuteration of the capric acid was performed by hydrothermal reactions using a Mini Benchtop 4560 Parr Reactor (600 mL vessel capacity, 3000 psi maximum pressure, 350 °C maximum temperature). Thin layer chromatography was used (referenced with the protonated compound) to estimate the purity and to develop separation protocols. ^{1}H (400 MHz) and ^{2}H NMR (61.4 MHz) spectra were recorded on a Bruker 400 MHz spectrometer at 298 K. Chemical shifts, in ppm, were referenced to the residual signal of the corresponding NMR solvent. Deuterium NMR was performed using the probe's lock channel for direct observation.

Electrospray ionization mass spectra (ESI–MS) were recorded for the deuterated fatty acid on a 4000 QTrap AB Sciex spectrometer. The overall percentage deuteration of the molecules was calculated by MS using the isotope distribution analysis of the different isotopologues. This was calculated taking into consideration the ^{13}C natural abundance, whose contribution was subtracted from the peak area of each M + 1 signal to allow for accurate estimation of the percentage deuteration of each isotopologue.

2.2. Synthesis of selectively deuterated tricaprin

The ^{1}H, ^{2}H and ^{13}C NMR spectra of all precursors and compounds used in this study are shown in the Supplementary information, Figs. SI1–SI16.

2.2.1. Deuteration of capric acid

The deuteration of the capric acid was achieved following a procedure published elsewhere (Salentinig et al., 2014). In summary, a mixture of the acid, Pt/activated carbon and NaOD in D_2O was subjected to two hydrothermal H/D exchange cycles in a Parr pressure reactor at 220 °C (23 bar) for 3 days each cycle. Purification of the deuterated compounds was performed on silica gel columns, eluted with the appropriate solvents.

2.2.2. Synthesis of 1,3-di-caproylpropane-2-one (1):

To a solution of 1,3-di-hydroxy acetone (2.9 g, 32.22 mmol), capric acid (11.1 g, 64.44 mmol) and *N,N′*-dicyclohexylcarbodiimide (DCC) (19.74 g, 64.44 mmol) was added dimethylaminopyridine (DMAP) (7.87 g, 64.44 mmol) in dichloromethane (250 mL) and stirred at room temperature for three days. The reaction mixture was filtered through a sintered funnel and washed with dichloromethane (3 × 50 mL). The filtrate was then evaporated under reduced pressure to give a pale yellow residue, which was purified by passing through a flash silica column using a 9:1 petroleum ether:ethyl acetate solvent to give a white crystalline substance 10.1 g 77% yield.

^{1}H NMR ($CDCl_3$): δ 0.87 (t, J = 6.51 Hz, 6H), 1.26–1.32 (m, 24H) 1.65 (m, 4H), 2.41 (t, J = 7.62 Hz, 4H), 4.74 (s, 4H).

^{13}C NMR ($CDCl_3$): δ 14.0, 22.6, 24.7, 29.0, 29.1, 29.2, 29.3, 31.8, 33.7, 66.1, 172.9, 198.1.

ESI–MS +ve m/z: 421 $(M + Na)^+$.

2.2.3. Synthesis of 1,3-di-caproylpropane-2-ol (2)

To a cold solution (10 °C) of **(1)** (2.8 g, 7.03 mmol) in THF:H_2O 15:1 (48 mL) was added sodium borohydride (0.43 g, 10.54 mmol) under nitrogen atmosphere. The reaction mixture was stirred at room temperature for 20 min and then poured into crushed ice (50 mL) and extracted with dichloromethane (3 × 50 mL). The combined extracts were dried over $MgSO_4$ and evaporated to give a gummy residue. This was purified by recrystallization from hexane to give a white crystalline solid in yield = 2.3 g, 82%.

^{1}H NMR ($CDCl_3$): δ 0.88 (t, J = 5.69 Hz, 6H), 1.26–1.32 (m, 24H) 1.63 (m, 4H), 2.35 (t, J = 7.56 Hz, 4H), 2.47 (d, 4.9 Hz, 1H (OH)), 4.06–4.21 (m, 5H).

^{13}C NMR ($CDCl_3$): δ 14.0, 22.6, 24.8, 29.0, 29.1, 29.4, 31.8, 34.1, 65.0, 68.4, 173.0.

ESI-MS +ve m/z: 423 $(M + Na)^+$.

2.2.4. Synthesis of sn-2 tricaprin-d_{19} (3)

This was prepared following the same procedure as reported for compound **(1)** (yield 88%). (Scheme 1)

^{1}H NMR ($CDCl_3$): δ 0.88 (t, J = 5.69 Hz, 6H), 1.27 (m, 24H) 1.60 (m, 4H), 2.31 (t, J = 7.56 Hz, 4H), 4.14 (dd, J = 5.86 Hz, 2H), 4.30 (dd, J = 5.68 Hz, 2H), 5.26 (m, 1H).

^{2}H NMR ($CDCl_3$): δ 0.78 (s, 3D), 1.17 (s, 11D), 1.51 (s, 2D), 2.23 (s, 2D).

^{13}C NMR ($CDCl_3$): δ 12.9, 14.0, 21.3, 22.6, 23.8, 24.8, 27.7, 27.9, 28.1, 29.1, 29.2, 29.4, 30.4, 31.8, 33.4, 34.0, 62.1, 68.8, 172.3, 173.3.

ESI-MS +ve m/z: 596 $(M + Na)^+$.

2.2.5. Synthesis of 1,3-di-caproylpropane-2-one-d_{38} (4):

Compound **(4)** was synthesized in a similar fashion to that of compound

(1) in 85% yield.

^{1}H NMR ($CDCl_3$): δ 0.87 (m, 0.13H), 1.26–1.32 (m, 0.48H) 1.95 (m, 0.08H), 2.41 (m, 0.13H), 4.74 (s, 4H).

^{2}H NMR ($CDCl_3$): δ 0.79 (s, 6D), 1.19 (s, 24D), 1.57 (s, 4D), 2.35 (s, 4D).

^{13}C NMR ($CDCl_3$): δ 13.0 (m), 21.3 (m), 23.7 (m), 27.8 (m), 30.5 (m), 32.9 (m), 66.1 (s), 172.9 (s), 198.1 (s).

ESI–MS +ve m/z: 459 $(M + Na)^+$.

2.2.6. Synthesis of 1,3-di-caproylpropane-2-ol-d_{39} (5):

Compound **(5)** was synthesized in a similar fashion to that of compound **(2)** in 88.5% yield (using sodium borodeuteride).

^{1}H NMR ($CDCl_3$): δ 0.81 (m, 0.10H), 1.22 (m, 0.40H) 1.56 (m, 0.07H), 2.30 (m, 0.13H), 2.57 (s, 1H (OH)), 4.11 and 4.17 (d,d, J = 11.6 Hz, 4H).

^{2}H NMR ($CDCl_3$): δ 0.79 (s, 6D), 1.19 (s, 23.3D), 1.54 (s, 3.84D), 2.27 (s, 3.86D), 4.04 (s, 1D).

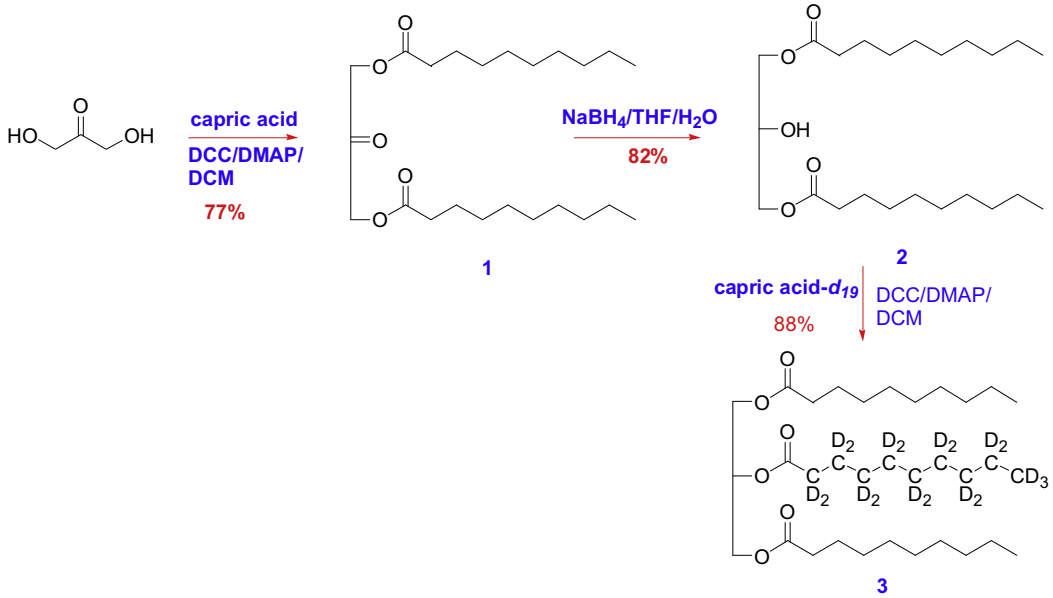

Scheme 1. Synthetic scheme for the preparation of *sn-1,3* tricaprin-d_{39} (**6**).

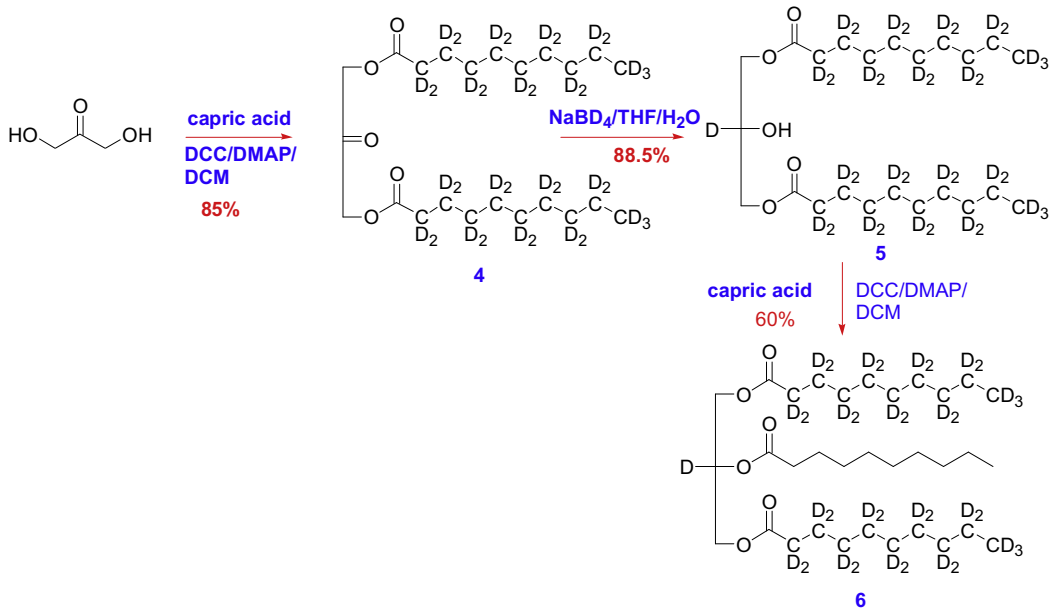

Scheme 2. Proposed pathway and chain migration occurring after 48 h of digestion of sn-2 deuterated tricaprin by pancreatic lipase at pH 6.5 and 37 °C showing the major and minor products observed by MS..

^{13}C NMR ($CDCl_3$): δ 13.2 (m), 21.3 (m), 23.7 (m), 27.8 (m), 30.5 (m), 33.6 (m), 66.1 (s), 67.9 (t), 173.9 (s).

ESI–MS +ve *m*/*z*: 462 $(M + Na)^+$.

2.2.7. Synthesis of sn-1,3 *tricaprin*-d_{39} ***(6)***

Compound **(6)** was synthesized in a similar fashion to that of compound **(3)** in 60% yield. (Scheme 2)

^{1}H NMR ($CDCl_3$): δ 0.87 (m, 3.26H), 1.26 (m, 13.0H) 1.61 (m, 2.67H), 2.31 (m, 2.24H), 2.57 (s, 1H), 4.13 and 4.28 (d,d, J = 12.0 Hz, 4H).

^{2}H NMR ($CDCl_3$): δ 0.78 (s, 6D), 1.17 (s, 23.3D), 1.51 (s, 3.67D), 2.23 (s, 3.78D), 5.20 (s, 1D).

^{13}C NMR ($CDCl_3$): δ 13.2 (m), 14.0, 21.3 (m), 22.6, 23.8 (m), 24.8, 27.8 (m), 29.0, 29.2, 29.4, 30.4 (m), 31.8 (s), 66.9 (s), 68.5 (t), 172.8 (s), 173.3 (s).

ESI-MS +ve *m*/*z*: 618 $(M + Na)^+$.

2.3. Methods

2.3.1. General

The emulsions containing 18 mM tricaprin were prepared in digestion buffer at pH 6.5 (100 mM PBS buffer with 150 mM NaCl) containing 2 mM bile salt (sodium taurodeoxycholate) as a stabilizer. Sonication with a tip sonicator for 3 min at 300 W was used to emulsify the components. The pH was adjusted to 6.5 using 1 M HCl and NaOH solution in the H_2O - or 1 M DCl and NaOD for the D_2O based emulsions. Pancreatin (2000 TBU in 0.1 mL of digestion buffer) was added to 10 mL tricaprin emulsion. Upon addition of the pancreatin, the pH-stat titrated the digestion mixture with 0.2 M NaOH for the H_2O based samples or NaOD for the D_2O based samples to maintain the system at pH 6.5.

2.3.2. Dynamic light scattering (DLS)

DLS was used to determine the mean hydrodynamic radius (R_H) and the width of the size distribution of the dispersed particles. Measurements were carried out on a Malvern Zetasizer NanoZS with a laser power of 4 mW at a back-scattering angle of 173° at 25 °C. Before the DLS measurements, all samples were centrifuged at 3500 rpm for 5 min and diluted 1/100 with MilliQ water to avoid multiple scattering effects. From the correlation functions, the average diffusion coefficient D was obtained by cumulant analysis (Pecora, 1985). The hydrodynamic radius R_H was deduced from the diffusion coefficient using the Stokes–Einstein equation:

$$R_H = \frac{k_B T}{6\pi\eta D} \quad (1)$$

k_B being the Boltzmann constant, T the absolute temperature (298.15 K) and h the viscosity of the solvent at this T (h (H_2O) = 0.890 cP). The polydispersity index (PDI) of the size distribution was determined from the second cumulant:

$$\mathrm{PDI} = \frac{\mu_2}{\overline{\Gamma}_2} \quad (2)$$

where μ_2 is the second cumulant and $\overline{\Gamma}$ the mean of the inverse decay time.

2.3.3. NMR spectroscopy

^{1}H NMR (400 MHz), and ^{2}H NMR (61.4 MHz) spectra of the deuterated *sn*-1,3 tricaprin in H_2O-based medium were recorded on a Bruker 400 MHz spectrometer at physiological temperature, 310 K, using a Wilmad® external reference NMR tube with ~50 μL $CDCl_3$ lock solvent. Chemical shifts, in ppm, were referenced to the residual signal of $CHCl_3$. Deuterium NMR was performed using the probe's lock channel for direct observation. ^{1}H NMR spectra of the completely protonated version of tricaprin in the D_2O-based medium was recorded using standard Wilmad® tubes and spectra were referenced to the residual signal of H_2O.

2.3.4. Mass spectrometry

Electrospray ionization mass spectra (ESI-MS) on a 4000 QTrap AB Sciex spectrometer were recorded for the digested triglycerides. Samples were diluted 20,000 times in an 1:1 methanol:water mixture. Enhanced MS positive mode was used to assess glyceride adducts and Enhanced MS negative mode was used to assess free

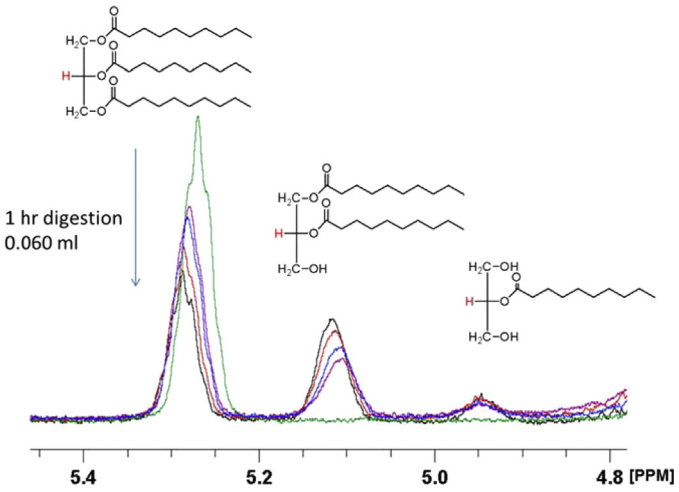

Fig. 1. *In-situ* ^{1}H NMR data during the digestion of protonated tricaprin at 37 °C and pH 6.5. The green curve was measured before lipase addition and the black curve after 1 h.

fatty acids. The optimized conditions were for both modes: declustering potential = +10 (−50), collision energy = 10 (−10), number of scans = 2, duration = 5 min, total scan time = 1.29 s, scan rate = 1000 Da/s.

3. Results and discussion

3.1. In situ NMR and DLS study of product formation during digestion

^{1}H and ^{2}H NMR experiments were used to study the digestion of protonated and specifically deuterated tricaprin under biologically relevant conditions (pH, T). ^{1}H spectra were recorded *in situ* during the digestion of protonated tricaprin, probing the characteristic chemical shift of the single hydrogen on the *C2* position of the glycerol backbone (see Fig. 1). Prior to the addition of pancreatic lipase, the spectra show characteristic patterns for tricaprin. The peaks are broadened as the triglycerides are emulsified, with a mean particle diameter of around 300 nm.

After addition of the lipase, the intensity of the triglyceride peak gradually decreases with the peak for diglyceride and monoglyceride appearing simultaneously. The chemical shift of the signal corresponding to the hydrogen on the *C2* position of the glycerol backbone shows that the lipase subsequently hydrolyses the ester bonds on the *sn-1* and *sn-3* position of the triglyceride leading to the *sn-2* monoglyceride and fatty acids. However, the relative peak intensities show that triglyceride and diglyceride are the dominating components during the first 1 h of reaction. The concentration of the *sn-1,2* dicaprin increased monotonically with the decrease of the tricaprin, while the concentration of the *sn-2* monocaprin remained relatively constant throughout the first hour of digestion. This suggests that *sn-2* monocaprin is present in equilibrium between two environments; dissolved in water as 'free' monocaprin, which NMR can detect as a distinct peak, and solubilized into colloids such as mixed micelles or vesicles, which hinders its detection by NMR. All NMR peaks disappeared upon completion of the digestion reaction after 3 h at pH 6.5, due to the self-assembly of the digestion products. The limited confinement for the monoglycerides and the fatty acids that are self-assembled into the bilayer of vesicles or micelles provides only limited degrees of mobility freedom for NMR to detect them. No significant concentrations of free glycerol could be detected. This was confirmed by spiking the NMR solution with small amount of glycerol to accurately identify the chemical shift of free glycerol signals in the medium. This indicates the stereoselectivity of the

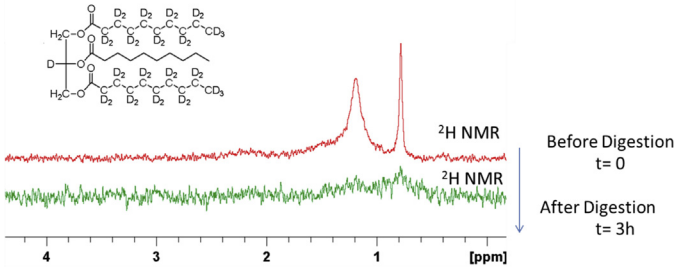

Fig. 2. ^{2}H NMR data of tricaprin emulsion containing fully deuterated fatty acid on *sn*-1/3 positions, before and after 3 h of pancreatic lipase digestion at 37 °C and pH 6.5. The broadening and disappearance of the NMR peaks (bottom spectrum) after 3 h indicates the hydrolysis of deuterated fatty acid chains and the formation of self-assembled aggregates (micelles or vesicles) of monoglyceride and free hydrolyzed fatty acids.

pancreatic lipase and shows that chain migration from the *sn-2* to *sn-1,3* positions in monoglycerides is negligible within the time frame relevant for lipid digestion. This was supported by probing the disappearance of the fatty acid chains on the *sn-1,3* positions when selectively deuterated *sn-1,3* tricaprin-d_{39} (compound **6)** was subjected to the same conditions and was probed by ^{2}H NMR. Within 3 h of digestion the labelled fatty acid chains at positions *sn-1* and *sn-3* disappeared from the spectrum (see Fig. 2).

The dynamic light scattering study of the mean particle size of the sample before and after digestion was in agreement with the interpretation of the NMR results: The transformation from initial oil droplets to colloidal structures is indicated by the decrease in correlation time and the corresponding R_H values from 244 nm (PDI 0.37) before digestion to 134 nm (PDI 0.40) after 3 h of digestion. The DLS correlation functions show rather monomodal particle size distribution for all samples (see SI Fig. SI17). This decrease in particle size and self-assembly structure formation is in agreement with results from triglyceride-emulsion digestions studied previously (Salentinig et al., 2011).

3.2. MS analysis of final digestion products

Mass spectrometry was used to analyze the products of tricaprin digestion directly after 3 h and 48 h of digestion. Selective deuteration of the capric acid chains on the triglycerides (*i.e.,* no deuteration, fully-deuterated capric acid chains on the *sn-2* position and fully deuterated chains on the *sn-1* and *sn-3* positions, in combination with deuteration of the hydrogen on the *C2* position on the glycerol backbone) provided detailed information on the reaction mechanism and stereospecificity of the lipase-catalyzed triglyceride digestion.

3.2.1. Digestion of the fully protonated tricaprin

MS measured after 3 h of digestion for fully protonated tricaprin presented in Fig. 3 shows *m*/*z* at 269.1 in positive mode MS which corresponds to $(M + Na)^+$ of monocaprin. Free glycerol was not detected above the noise level at *m*/*z* 115 $(M + Na)^+$. No dicaprin (*m*/*z* 423.3 $(M + Na)^+$) or tricaprin (*m*/*z* 557.4 $(M + Na)^+$ were observed (see Fig. 3). This shows that complete digestion of the tricaprin occurred which terminated at monocaprin and did not proceed further to free glycerol. The same sample showed a peak at *m*/*z* 171.1 in negative mode MS which corresponds to $(M - 1)^-$ of capric acid (see Fig. 3)

The spectrum recorded after 48 h digestion (see Fig. SI 18) showed the same results. No free glycerol was detected (a signal below the noise level at *m*/*z* 115 for $(M + Na)^+$). This agrees with the results from the NMR, and the fact that free glycerol was not detected by NMR or MS suggests that no significant isomerization

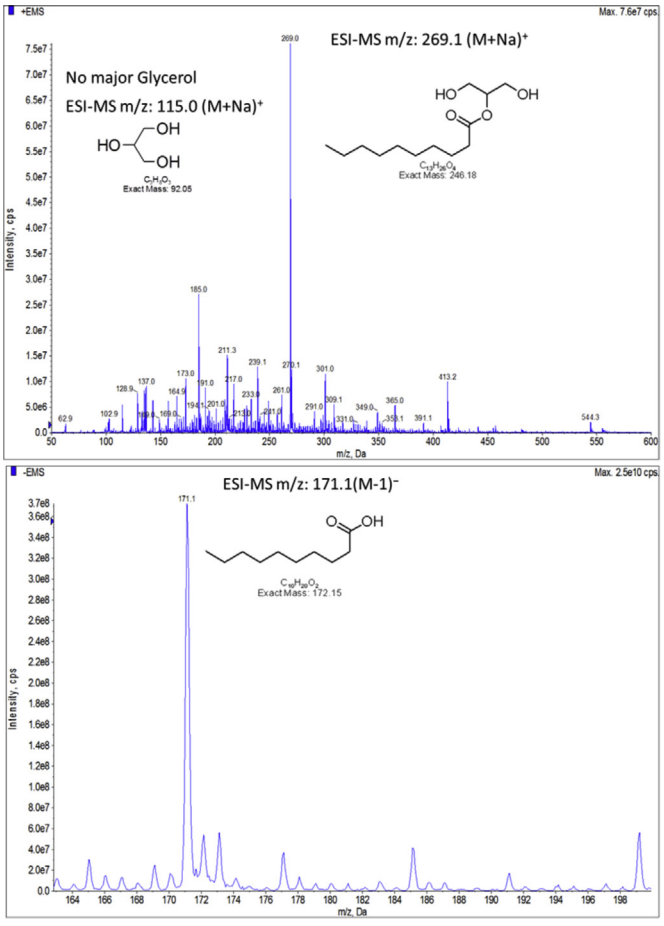

Fig. 3. MS data of the tricaprin emulsion after 3 h of lipase action at pH 6.5 and 37 °C in positive (top) and negative mode (bottom).

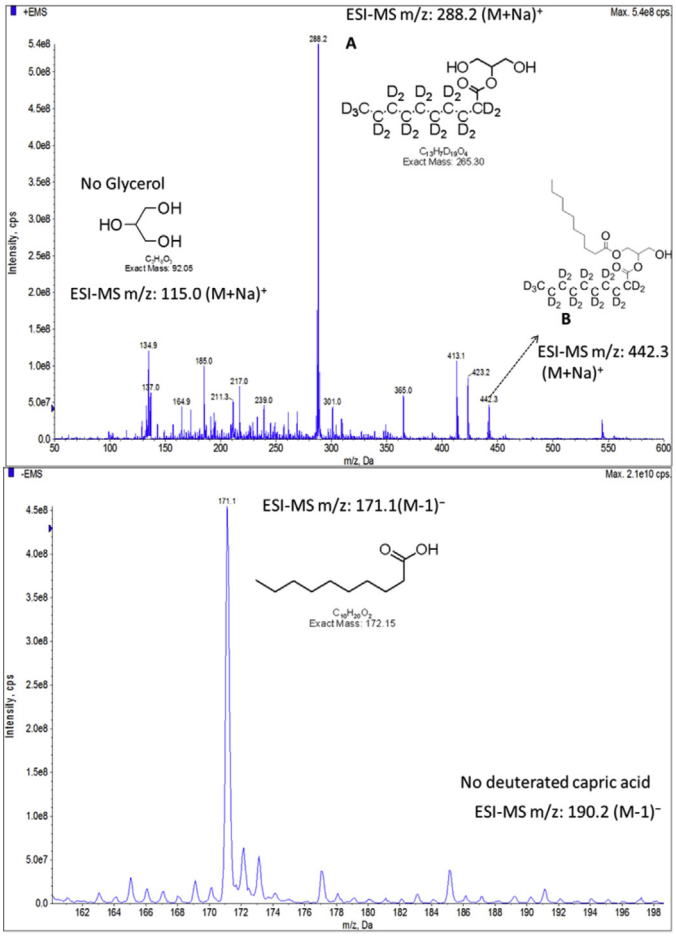

Fig. 4. MS data for the tricaprin emulsion containing fully-deuterated fatty acids on the *sn-2* position after 3 h of lipase action at pH 6.5 and 37 °C in positive (top) and negative mode (bottom).

or fatty acid migration from the *sn-2* monoglyceride to *sn-1* or *sn-3* monoglyceride occurs under the conditions of this study; if this were indeed the case, lipase hydrolysis should have acted upon these glyceride positions and produced free glycerol as the final product. These results are in contrast to the acyl migration of ~30% reported for *sn-1,2* diglycerides after 24 h at 37 °C (Kodali et al., 1990). The presence of bile salt and free fatty acids in addition to the monoglyceride in the simulated intestinal fluid, leads to self-assembly into colloidal structures. Thus the results from the *in-vitro* digestion agree with the reported increase in chemical stability of the *sn-2* monoglyceride in such structures (Kodali et al., 1990; Holmberg and Osterberg, 1988; Holmberg and Österberg, 1990; Mazur et al., 1993). The self-assembly of the *sn-2* monoglycerides to form colloidal structures makes the molecule more thermodynamically stable and hence prevent acyl migration. Usually small chain glycerides display faster rates of acyl migrate than long chain ones but the presence of self-assembled colloidal structures of the partially hydrolyzed lipids plays a major role in the prevention of acyl migration and further hydrolysis of the sn-2 monoglycerides.

To confirm the identity of the digestion products and to determine the pathways of any migration that may have occurred during the digestion process, selectively deuterated tricaprin and MS analysis was used.

3.2.2. Digestion of the sn-2 deuterated tricaprin (3)

After 3 h digestion of tricaprin with deuterated capric acid at the *sn-2* position, peaks were observed at *m/z* 288.2 in positive mode MS, which corresponds to $(M+Na)^+$ of *sn-2* deuterated monocaprin. No peak was observed at *m/z* 270.1, corresponding to hydrogenated monocaprin (see Fig. 4). A small amount of *sn-1,2* dicaprin (deuterated in one chain, *sn-2*) was observed at *m/z* 442.3 $(M+Na)^+$, suggesting a low extent of incomplete digestion of the tricaprin (initial concentration of 18 mM). No other digestion products of tricaprin nor their Na^+ adducts were found, and glycerol was not detected (absence of the peak at *m/z* 115.0 $(M+Na)^+$). The spectrum recorded in negative mode shows a peak at *m/z* 171.1 corresponding to $(M-1)^-$ of hydrogenated capric acid. No deuterated capric acid was observed. The selective deuteration of the capric acid on the *sn-2* position of the tricaprin confirms the stereospecificity of pancreatic lipase hydrolysing only the *sn-1* and *sn-3* positions but not the *sn-2* position (*i.e.*, the presence of *sn-2* deuterated monocaprin only and the absence of free deuterated capric acid).

The spectrum after 48 h of digestion of *sn-2* deuterated tricaprin showed *m/z* at 288.2 in positive mode MS which corresponds to $(M+Na)^+$ of *sn-2* monocaprin only. A small peak (**A′**) at *m/z* 269.0 $(M+Na)^+$ (see Fig. SI 19) from non-deuterated *sn-2* monocaprin was observed suggesting that the small amount of the *sn-1,2* dicaprin (**B**) that was present undigested after 3 h had rearranged to *sn-1,3* dicaprin (**B′**) as illustrated in Scheme 3. The proposed pathway was confirmed by the presence of some deuterated capric acid in the MS negative mode (Fig. SI 19). Free glycerol was also observed in very limited amount at *m/z* 115 $(M+Na)^+$. The composition of the sample after 48 h digestion shows that chain migration from the *sn-2* to the *sn-1/3* position occurs which leads

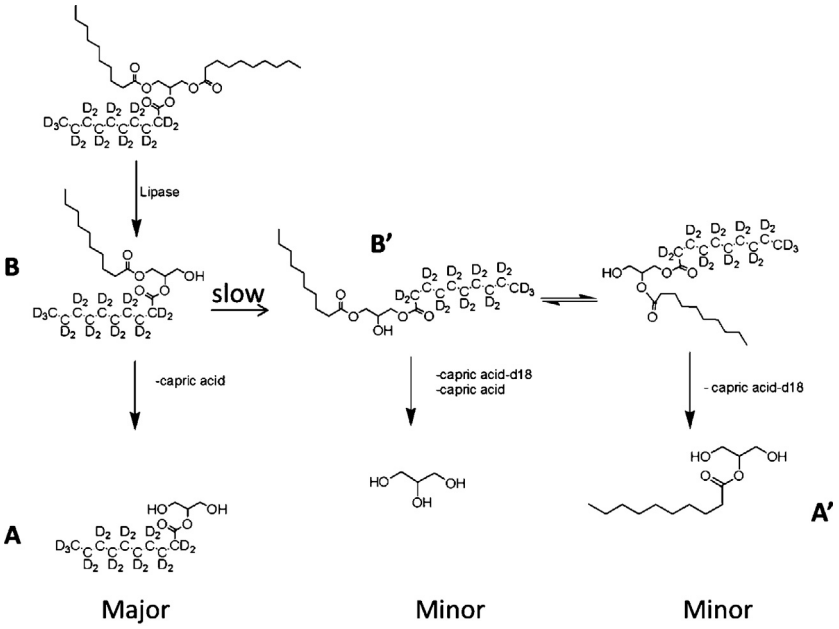

Scheme 3. Synthetic scheme for the preparation of *sn-2* tricaprin-d_{19} (**3**).

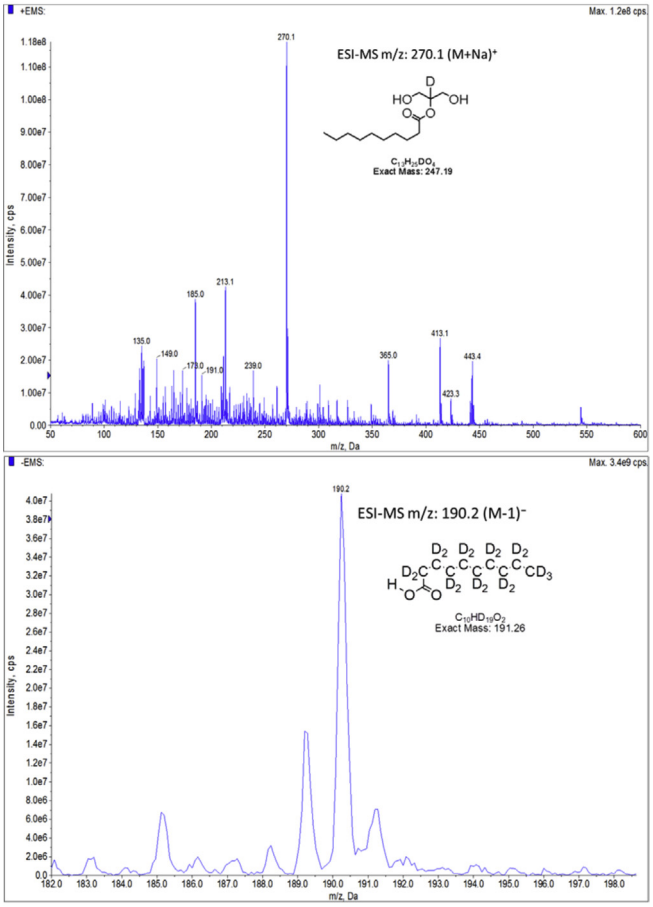

Fig. 5. MS data for *Sn-1,3* deuterated tricaprin after 3 h of digestion at 37 °C at pH 6.5.

to complete digestion. However, this process is very slow under the simulated *in vivo* conditions of this experiment given the small amounts detected by MS, and will only occur due to the presence of small traces of undigested dicaprin (**B**) in the digestion medium for long periods of time (48 h).

3.2.3. *Digestion of the* sn-1,3 *deuterated tricaprin*

The digestion of the *sn-1,3* tricaprin containing deuterated capric acid on the *sn-1* and *sn-3* positions with additional deuterium atom on the *C2* of the glycerol backbone provides further complementary information on the stereospecificity of the tricaprin digestion reaction and supports the illustration presented in Scheme 3. MS measured after 3 h of digestion of this component showed *m/z* at 270.1 in positive mode MS which corresponds to $(M+Na)^+$ of *sn-2* monocaprin with protonated fatty acid (see Fig. 5). Free glycerol-d was not detected above the noise level at *m/z* 116 $(M+Na)^+$ confirming that digestion to glycerol does not occur in significant amounts within this biologically relevant timeframe. To confirm the absence of free glycerol, and to address any detection issues including detection limits of MS, an equimolar amount of free glycerol to the initial tricaprin was injected into the above 3 h digested mixture. This showed the expected peak *m/z* 115 in MS corresponding to the spiked glycerol (see Fig. SI 20) but no *m/z* 116 was observed which corresponds to glycerol-d which could have come from the complete digestion of *sn-1* and *3* deuterated tricaprin. Traces of dicaprin (*m/z* 443.4 $(M+Na)^+$) were observed indicating some incomplete digestion after 3 h as was observed before. In negative mode MS, digestion of *sn-1,3* deuterated tricaprin showed *m/z* at 190.2 which corresponds to $(M-1)^-$ of capric acid-d_{19}, and no protonated capric acid was observed. The free *deuterated* fatty acids shift by a significant +19 on the *m/z* scale relative to the protonated fatty acid, in agreement with the ^2H content. This provides direct determination of position of the cleaved ester bond on the triglyceride (see Fig. 5).

The spectrum recorded after 48 h of digestion is presented in Fig. SI 21. This spectrum shows a peak at *m/z* 270.1 in positive mode MS which corresponds to $(M+Na)^+$ of *sn-2* protonated

monocaprin. Traces of *sn-2* deuterated monocaprin were also observed at *m*/*z* 289.2 $(M+Na)^+$ with very limited amount of glycerol-d at *m*/*z* 116 $(M+Na)^+$; this suggests that upon longer digestion time the small amount of *sn-1,2* dicaprin had rearranged to *sn-1,3* dicaprin as illustrated in the digestion of the *sn-2* deuterated tricaprin (**3**) in Scheme 3.

4. Conclusion

In-situ NMR and mass spectrometry, in combination with selectively deuterated tricaprin, were used to study the stereo-specificity and chain migration during the digestion of tricaprin under biologically relevant conditions. This study focused on the reaction mechanism and self-assembly of reaction products of the medium chain triglyceride under conditions similar to the human small intestine. NMR and dynamic light scattering showed that the tricaprin digestion products *sn-2* monocaprin and capric acid in combination with the bile salt self assemble into colloidal structures. To investigate the influence of self-assembly structure formation on the thermodynamic stability of the *sn-2* monocaprin, the reaction mechanism was further investigated using in-situ NMR and mass spectrometry in combination with selectively deuterated tricaprin. Deuterium labeling is highly beneficial in extending the use of mass spectrometry and NMR to determine reaction mechanism and identify products that have similar molecular masses of large systems such as the self-assembled colloidal structures formed during the triglyceride digestion. All methods showed the formation of *sn-2* monoglyceride and fatty acids and the formation of glycerol was not observed. Evidence of some chain migration was observed but this remained very limited and was attributed to the presence of traces of undigested diglycerides after 3 h of digestion. The chain migration from the *sn-2* to the *sn-1* position is slow under the biologically relevant conditions of this study (temperature, pH). As biologically relevant times for digestion of lipids in humans are around 3 h, the majority of the products resulting from tricaprin digestion are the *sn-2* monocaprin and free capric acid. These results are also important in industrial processes that utilize lipase technology for the modification of oils and fats to produce high-value added products, such as cocoa butter equivalents, human milk fat substitutes, and other specific-structured lipids.

Acknowledgements

The authors would like to thank the Australian Institute for Nuclear Science and Engineering (AINSE Ltd.) for providing financial assistance (ALNGRA14052). Parts of this study were funded by the Australian Research Council through the Discovery Projects scheme (DP120104032). The National Deuteration Facility is partially funded by the National Collaborative Research Infrastructure Strategy, an initiative of the Australian Federal Government.

Appendix A. Supplementary data

Supplementary data associated with this article can be found, in the online version, at http://dx.doi.org/10.1016/j.chemphyslip.2015.06.007.

References

Akoh, C.C., Xu, X., 2002. Lipid Biotechnology. In: Kuo, T.M., Gardner, H.W. (Eds.), Marcel Dekker, Inc., New York, pp. 461–469.
Austin, M.A., 1991. Arterioscler. Thromb. Vasc. Biol. 11, 2.
Bach, A.C., Babayan, V.K., 1982. Am. J. Clin. Nutr. 36.
Borgström, B., 1964. J. Lipid Res. 5, 522.
Boswinkel, G., Derksen, J.T.P., van't Riet, K., Cuperus, F.P., 1996. J. Am. Oil Chem. Soc. 73, 707.
Compton, D., Vermillion, K., Laszlo, J., 2007. J. Am. Oil Chem. Soc. 84, 343.
Hayes, K.C., 2001. Curr. Opin. Lipidol. 12, 55.
Hernell, O., Staggers, J.E., Carey, M.C., 1990. Biochemistry 29, 2041.
Hofmann, A.F., Borgström, B., 1964. J. Clin. Invest. 43, 247.
Holmberg, K., Österberg, E., 1990. Surfactants macromolecules: self-assembly at interfaces and in bulk. Prog. Colloid Polym. Sci. 82, 181.
Holmberg, K., Osterberg, E., 1988. J. Am. Oil Chem. Soc. 65, 1544.
Katan, M.B., 2000. Nutr. Rev. 58, 188.
Kodali, D.R., Tercyak, A., Fahey, D.A., Small, D.M., 1990. Chem. Phys. Lipids 52, 163.
Laszlo, J., Compton, D., Vermillion, K., 2008. J. Am. Oil Chem. Soc. 85, 307.
Mazer, N.A., Benedek, G.B., Carey, M.C., 1980. Biochemistry 19, 601.
Mazur, A.W., Burns, J.L., Hiler, G.D., Spontak, R.J., 1993. J. Phys. Chem. 97, 11344.
Narayanan, V.S., Storch, J., 1996. Biochemistry 35, 7466.
Pecora, R., 1985. Dynamic Light Scattering. Plenum Press, New York.
Salentinig, S., Sagalowicz, L., Glatter, O., 2010. Langmuir 26, 11670.
Salentinig, S., Sagalowicz, L., Leser, M.E., Tedeschi, C., Glatter, O., 2011. Soft Matter 7, 650.
Salentinig, S., Phan, S., Khan, J., Hawley, A., Boyd, B.J., 2013. ACS Nano 7, 10904.
Salentinig, S., Phan, S., Darwish, T.A., Kirby, N., Boyd, B.J., Gilbert, E.P., 2014. Langmuir 30, 7296.
Salentinig, S., Phan, S., Hawley, A., Boyd, B.J., 2015. Angew. Chem. Int. Ed. 54, 1600.
Schurtenberger, P., Mazer, N., Kaenzig, W., 1985. J. Phys. Chem. 89, 1042.
Unger, R.H., Zhou, Y.T., 2001. Diabetes 50, S118.
Voet, D., Voet, J.G., 1995. Biochemistry. Wiley.
Xu, X., 2000. Eur. J. Lipid Sci. Technol. 102, 287.